Ultrasound internal tattooing

Olivier Couture[a)] and Magalie Faivre
ESPCI, Paris 75005, France; Fondation Pierre-Gilles de Gennes, Paris 75005, France; and CNRS, France

Nicolas Pannacci
ESPCI, Paris 75005, France

Avin Babataheri
ESPCI, Paris 75005, France

Vincent Servois
Institut Curie, Paris 75005, France

Patrick Tabeling
ESPCI, Paris 75005, France and CNRS, France

Mickael Tanter
ESPCI, Paris 75005, France; CNRS, France; and INSERM, France

(Received 26 July 2010; revised 3 January 2011; accepted for publication 4 January 2011; published 1 February 2011)

Purpose: The ability of remotely tagging tissues in a controlled and three-dimensional manner during preoperative imaging could greatly help surgeons to identify targets for resection. The authors' objective is to selectively and noninvasively deposit markers under image guidance for such internal tattooing.
Methods: This study describes the production of new ultrasound-inducible droplets carrying large payloads of fluorescent markers and the *in vivo* proof of concept of their remote and controlled deposition via focused ultrasound. The droplets are monodispersed multiple emulsions produced in a microfluidic system, consisting of aqueous fluorescein in perfluorocarbon in water. Their conversion (either by vaporization or cavitation) is performed remotely using a clinical ultrasonic imaging probe.
Results: When submitted to 5 MHz imaging pulses, the droplets vaporize *in vitro* at 1.4 MPa peak-negative pressure and eject their content. After several seconds, a brightly fluorescent spot (0.5 mm diameter) is observed at the focus of the transducer. Experiments in the chorioallantoique membrane of chicken eggs and chicken embryo demonstrate that the spot is stable and is easily seen by naked eye.
Conclusions: These ultrasound-inducible multiple emulsions could be used to deliver large amounts of contrast agents, chemotherapy, and genetic materials *in vivo* using a conventional ultrasound scanner.
[DOI: 10.1118/1.3548068]

Key words: sonoporation, ultrasound, surgery, multiple emulsion, microfluidics

I. INTRODUCTION

The spatial concordance between a lesion depicted in a radiological image and its localization in the operating room is still a major issue in therapy. As the sensitivity of medical imaging modalities is constantly improving, clinicians are now increasingly confronted with tumors that are detected by the imaging device but which remain invisible and impalpable during surgery. Furthermore, the very success of preoperative chemotherapy often reduces the contrast of metastasis, even when they are still malignant.[1] These issues with tumor localization force the resection of wide margins of healthy tissue, causing functional impairment to patients who are already weakened by their treatments or possible relapse.

Tumor tracking methods are frequently used to help surgeons during the intervention. The simplest methods consist in implanting a foreign object (hook, clip, or gold rod[2]) or injecting a marker near or inside the tumor.[3,4] These invasive procedures require puncturing the skin and are limited to accessible locations. Moreover, guiding tools do not determine the outline of the tumor, but rather its approximate position.

More complex methods such as image registration are also exploited during surgery. Virtual models based on radiology can be projected on images of the patient during surgery.[5] Although these projections are appropriate in static conditions such as the skull, they are affected by motion and deformation of soft tissue.[6] This problem can be partly circumvented by the real-time superposition of the operatory field's images and those obtained by an advanced optical system which highlights fluorescent markers.[7] This method

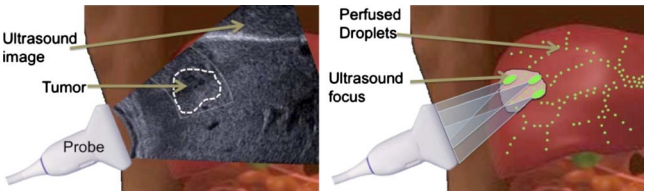

FIG. 1. Principle of the internal tattooing: The diseased tissue is identified by medical imaging (magnetic resonance imaging, computed tomography, ultrasound, or x ray) and then the droplets are injected intravenously. The release of the optical marker is induced and tracked by focusing ultrasound pulses in the tissue to be resected. The defined zone then becomes observable by sight.

has been used for the detection of sentinel nodes in breast cancer patients,[8] but it is dependent on the biodistribution of the dye in the body.

Surgeons are confronted with many forms of cancer (primary tumor, nodes, and metastasis in various organs) and they require a simple and robust system that can link the information from the preoperative imaging to the operating field, which still mostly relies on sight. For this purpose, we propose the concept of internal tattooing activated by focused ultrasound. Beyond its extremely precise spatial control, a key advantage of this approach lies in the fact that such tattooing is activated during ultrasonic imaging by the same conventional probe that performs the patient's exam. This ensures the perfect collocation between the ultrasonic radiological image and the spatial localization of optical markers *in situ*.

The objective of this study is to deposit large quantities of optical markers at a precise location, which could then be identified during surgery. We propose to use novel injectable droplets carrying important payloads of contrast agent and that are inducible by ultrasound. These droplets can be converted by vaporization or by cavitation induced by focusing the ultrasound energy in a targeted region defined on the radiological images. The release of the marker is combined to the effect of sonoporation that can drive the optical markers within the medium outside the blood vessels.[9] A tissue to be resected can thus be painted point-by-point with a submillimeter resolution corresponding to the size of the focal spot of the ultrasound system (see principle in Fig. 1).

Various ultrasound-inducible objects have been previously developed for drug delivery. Previous designs implied, in most cases, functionalizing the membrane of microbubbles or gas-precursor particles.[10] However, tattooing a region to be seen by the naked eye requires very large payloads of marker incompatible with such approaches. We thus proposed a new composite droplet which carries the marker within a nanoemulsion that comprise at least two-thirds of its volume.[11] The droplet's matrix is formed of perfluorocarbon oil, which acts as a barrier isolating the content of the droplet from the external medium. The oil is converted when subjected to an ultrasound pulse of sufficient intensity and thus forces the delivery of the content of the compound droplet in the external medium. Such liquid perfluorocarbon have been used by several groups for ultrasound-induced droplet vaporization for imaging[12] and therapeutic purposes.[13–18] To guarantee that they all behave similarly toward the ultrasound release system and to avoid embolism, the droplets are generated in a dedicated microfluidic device, which ensures monodispersity (below 3%) and small sizes (below 5 μm).

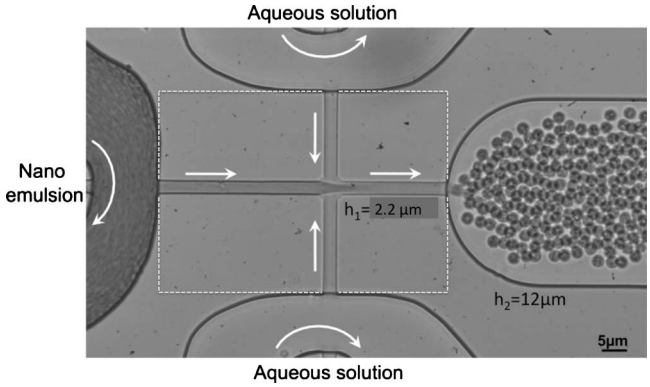

FIG. 2. The nanoemulsion (left channel) was encapsulated in micron-sized droplets via a microfluidic device. The typical channel height was chosen to be 2.2 μm in the narrow region and 12 μm for the wide channels. The droplets were formed at the step between the shallow and deep channels. The dashed arrows represent the flow direction of each phase. The dashed rectangle represents the border between the two different heights.

The paper describes the generation of the composite emulsions, their ultrasound-induced conversion, and the *in vitro* tattooing, along with *in vivo* proof-of-principle in the chicken embryo.

II. MATERIALS AND METHODS

II.A. Fabrication of the droplets

The droplets were fabricated in two steps: The formation of a primary nanoemulsion and then its encapsulation in a micron-sized drop. The primary emulsion consisted in an aqueous solution saturated with fluorescein (approximately 3% w/w), dispersed in low-boiling point perfluorocarbon (perfluorohexane), and stabilized by a fluorinated surfactant (Krytox, 2.9% w/w of perfluorocarbon phase).[19] The nanoemulsion is obtained using a rotor-stator homogenizer (Polytron, Kinematica, Switzerland); the typical diameter of the droplets in the primary emulsion could be reduced to hundreds of nanometers. After centrifugation, the volume fraction of water is predicted to be higher than two-thirds for closely packed polydisperse spheres.

The nanodroplets were then encapsulated as micron-sized droplets in water via a microfluidic device, using the principle of the step emulsifier described in Ref. 20. The design of the microfluidic system for producing microdroplets in an aqueous solution is described in Fig. 2. The system was made of polydimethylsiloxane. The channels heights, which determined the size of the composite drops produced, were chosen to be 2.2 and 12 μm. The nanoemulsion and the water were pushed through the system with air pressures of 2.5 and 1 bar, respectively. A total of 2500 droplets were generated every second as measured by high-speed microscopy. The nanoemulsion was stabilized by Pluronic®

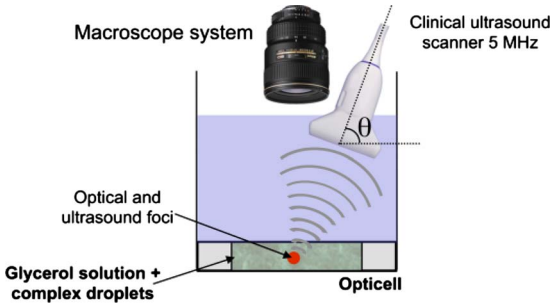

FIG. 3. Setup for the *in vitro* release of fluorescein from the composite particles in an Opticell plate. The clinical ultrasound probe is placed with an angle $\theta=50°$ relatively to the Opticell plate, whereas the camera is set at the vertical of the ultrasound focus.

(polyoxyethylene-polyoxypropylene block copolymer, Sigma-Aldrich, St. Louis, MO, 1% w/w of the total solution). The droplets were collected and used within 48 h.

II.B. *In vitro* ultrasound release

The composite drops were diluted in an aqueous solution of glycerol (35% w/w) and injected in an Opticell plate made of two plastic membranes, transparent to both ultrasound and light, separated by 2 mm (Fig. 3). The bottom membrane was placed at the foci of a macroscope (magnification=5×) and of a 5 MHz ultrasound probe (128 elements, pitch 0.3 mm), which was immersed in water at room temperature. The ultrasonic probe was driven by a clinical ultrasound scanner (Supersonic Imagine, Aix-en-Provence, France), which generated images of the medium underneath the probe. Release spots could then be selected anywhere on the image through software. Short emission sequences were then implemented to focus ultrasound pulses (1–5 cycles, 0.8–2.5 MPa peak-negative pressure) at these locations by controlling the delays on each electronic channel. After each focused pulse (150 μs), an ultrafast image[21] was generated to track the effect of the release. A differential image was used to map the changes in the ultrasound signal due to the conversion of the droplets over the following 15 ms. Concurrently to the ultrasound imaging, a series ($n=15$) of macroscopic fluorescent images were obtained of the focus spot over 10 s. Fluorescein was excited by blue light (470 nm) and it was imaged with an orange photographic filter (cutoff: 520 nm).

II.C. *In vivo* ultrasound release

The release of optical markers was also tested *in vivo* in 8–10 days old chicken embryos. In the first set of experiments, the embryo was kept in the shell where an acoustic and optical window was created by removing part of the shell. The injection of the droplets was made in a large vein of the chorioallantoic membrane (CAM). The droplets were injected in the CAM via a catheter at a flow rate of 100 μl/min thanks to a syringe pump (Harvard Apparatus, Holliston, MA). The egg was then immersed in water and a 3.5 MPa peak-negative pressure was induced in the CAM at a different position than the injection site [see Fig. 4(a)]. Finally, the egg was illuminated with blue LEDs (470 nm) and fluorescence was observed through appropriate filters on goggles and on a photographic camera.

Another set of experiments was performed where the embryo attached to the CAM was separated from the shell and disposed in a Petri dish; 100 μl of the droplets suspension were injected via an intracardiac injection with a catheter. The embryo was then immersed in water and ultrasound

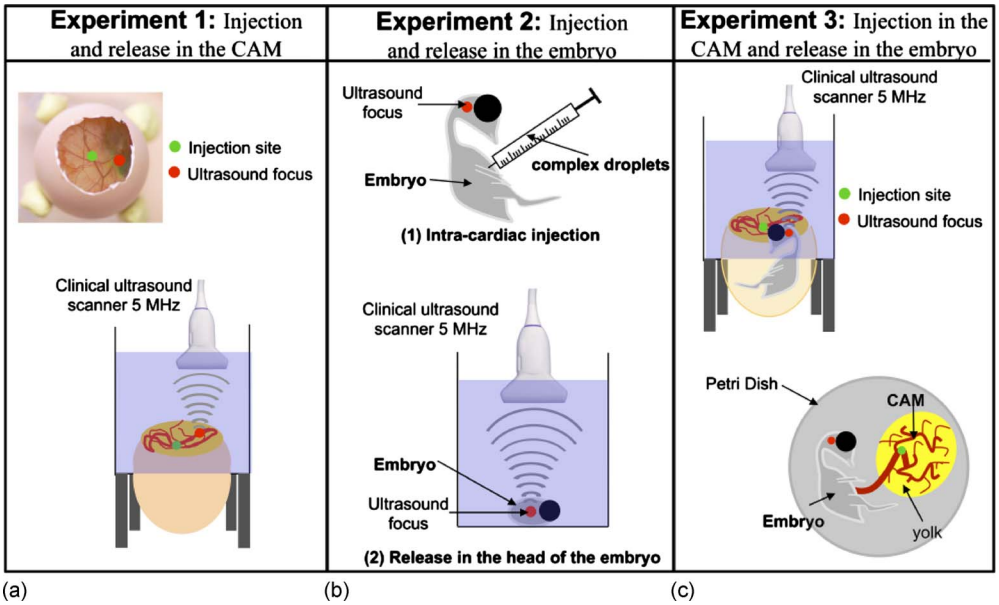

FIG. 4. Setup for the *in vivo* release of fluorescein from the composite particles in a chicken embryo. The same ultrasonic system than previously was transposed to the *in vivo* experiments. (a) The injection of the droplets and the release are realized in the CAM of the chicken embryo. (b) In another set of experiments, the injection and the release were done in the embryo itself. In a first step, the complex droplets were injected via intracardiac puncture. Then the ultrasound pulse was directed on the embryo's head to induce the release. (c) Finally, the injection of the droplets was made in the CAM, whereas the deposit of the fluorescein is induced in the embryo. The observation was made both in the egg and in a Petri dish.

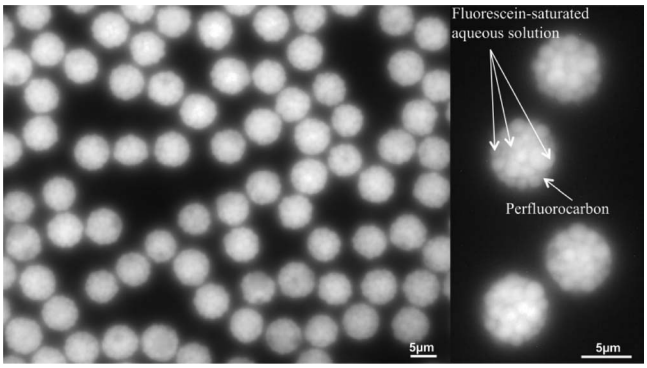

FIG. 5. Composite microdroplets observed under epifluorescent microscopy (exposure time=2 s). The emulsion consisted of water saturated with fluorescein encapsulated in a vaporizable liquid perfluorocarbon drop suspended in an aqueous media.

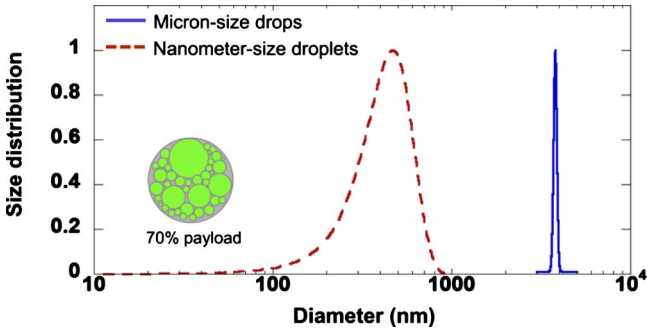

FIG. 6. Size distributions of the nanoemulsion, as measured by dynamic light scattering, and of the composite micron-sized droplets, as measured with microscopy. The polydispersity of the nanoemulsion allowed a large payload (70%) within the micron-sized droplets, whereas the diameter of the micron-sized droplets was smaller than 4 μm and very well controlled (coefficient of variation $<3\%$).

pulses (3.5 MPa) were focused at two spots separated by 2 mm on the head of the embryo. Finally, the embryo was illuminated with blue LEDs (470 nm) and fluorescence was observed through appropriate filters on goggles and on a photographic camera.

Finally, in the last set of experiments, the embryo was kept in the shell where a part was removed. The injection of the droplets (150 μl) was made in a large vein of the CAM and the release of the optical marker was induced in the embryo itself [as presented in Fig. 4(c)]. The egg was immersed entirely in water and a 3.5 MPa peak-negative pressure was focused near the eye of the embryo [see Fig. 4(c)]. The egg was illuminated with blue LEDs (470 nm) and fluorescence was observed through appropriate filters on goggles and on a photographic camera. Finally, the embryo attached to the CAM was separated from the shell and disposed in a Petri dish for further observation.

III. RESULTS

III.A. Double-emulsion droplets production

Nanometer-sized drops of optical markers were dispersed in a solution of fluorinated oil. This nanoemulsion was then encapsulated as micron-sized droplets in water in a dedicated microfluidic device (see Sec. II). Figure 5 shows a typical high magnification epifluorescent picture of the composite droplets produced in the microfluidic system. Brightly fluorescent droplets of fluorescein (captured with a long exposure time=2 s) surrounded by perfluorohexane could be distinguished in the water suspension. The nanoemulsion, measured by dynamic light scattering (Malvern Zetasizer, Malvern Instruments, Malvern, UK), was found to cover a wide range of sizes with a peak at 400 nm (Fig. 6). The composite droplets, measured with a microscope, were found to be monodisperse, their diameters being equal to 3.80 ± 0.14 μm.

III.B. *In vitro* study of the ultrasound-triggered release

We first investigated the influence of the different acoustic parameters on the fluorescein delivery process. The composite droplets were suspended in a glycerol solution (35% w/w) to mimic the viscosity of blood. They were introduced uniformly at a concentration of 1.5% v/v in an Opticell chamber, which is transparent to both light and ultrasound. Ultrasound pulses were focused in a submillimetric region of the plate using a multielement medical imaging probe. An ultrasound movie of the release process was created from a series of images obtained after each focused pulse. The ultrasound release sequence was performed in less than 20 ms.

Before the initiation of the ultrasound ($t=0$), no fluorescent signal arose from the composite droplets (exposure time=250 ms). This is due to optical quenching of the fluorophores present at large concentrations within the nanoemulsion.[22] When the 3.5 MPa peak-negative pressure pulses were initiated, a sudden burst was observed. The fluorescein content in the drops appeared to be propelled over several hundreds of microns, giving rise to the fish structure displayed in Fig. 7. Further on, as the molecules of fluorescein slightly diffused in the surrounding fluid, local concentrations of the fluorophores decreased, thus removing optical

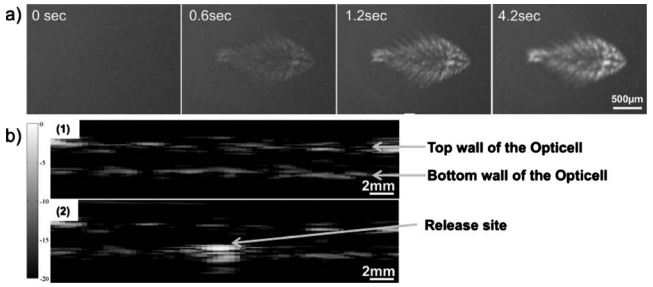

FIG. 7. (a) Time sequence of fluorescein release upon ultrasound pulse application at the macroscopic scale. Initially ($t=0$), there was no evident fluorescence; then, application of ultrasound-induced the perfluorocarbon conversion ($t=0.6$ s). After its release, fluorescein diffused in the surrounding medium ($t=1.2$ and 4.2 s). (b) Ultrafast ultrasound imaging of the droplet's conversion. The focused ultrasound pulses are targeted to the center of the image, corresponding to the bottom of the Opticell plate where the droplets have sedimented. (i) Image obtained 150 μs prior to conversion; (ii) 150 μs after.

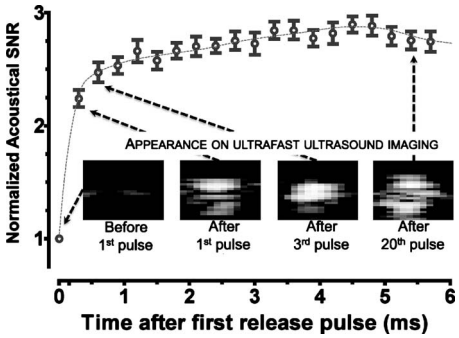

FIG. 8. Ultrasound imaging of the release in the Opticell plate at 3200 images/second (inset) and evolution of the acoustic SNR during the release sequence. The first impulsion creates a highly echogenic target at the focus of the ultrasound release pulse, over a region that contained several droplets before release. This hyperechoic region persists for the duration of the release. The width of each image is 3.3 mm and it is centered at the focus point of the release ultrasound.

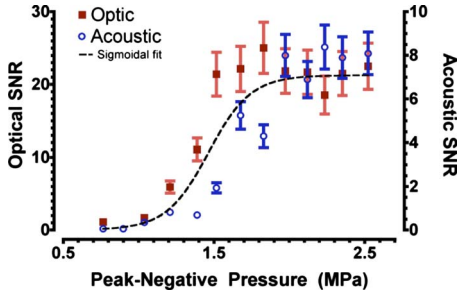

FIG. 9. Release of the marker at different ultrasound intensities as detected by the optical camera and the ultrasound imaging sequence. SNR is calculated with respect to the background signal prior to the release on both optical and ultrasound images. Relative error bars have been estimated through 20 repetitions of the same set of parameters. The fit is a Boltzmann sigmoidal. The threshold for release is assessed from the peak-negative pressure at half-maximum (P50). The optic threshold is 1.35 ± 0.04 MPa and the acoustic threshold is 1.68 ± 0.06 MPa.

quenching phenomenon, and fluorescein became increasingly visible. The formation of gas bubbles was observed at the site of the release.

Parallel to the optical observation, ultrafast ultrasound imaging (3200 images/second) was performed to track changes linked to the release of the droplets.[23] Images acquired 150 μs before the focused high-intensity pulse do not highlight any signal in the culture plate except the two parallel membranes forming the boundaries of the plate. Just after the focused releasing pulse (150 μs), the ultrasonic imaging displayed an important contrast in the region where the ultrasound pulses were focused. This hyperechoic region evolved over the several milliseconds after the initiation of the release highlighting the interest of very high ultrasonic frame rates for the imaging of the markers deposit (Fig. 8).

Ultrasound release was tracked optically and ultrasonically for focused acoustic pulses of various amplitudes (peak-negative pressure in MPa). Optical signal to noise ratio (SNR) was determined based on the intensity of the fluorescence generated in the focal zone after release. Acoustic SNR was obtained from the variation of the echo intensity backscattered from the focus. The acoustic SNR attained rapidly a saturation point [Fig. 8], demonstrating that a single pulse of ultrasound (two cycles) can deliver the content of the droplet. As shown in Fig. 9, both measurements demonstrated that the delivery process is associated to well defined acoustic threshold conditions, centered around 1.5 MPa for 5 MHz pulses. This threshold varied with the frequency (Fig. 10) and attained a maximum efficiency at the lower edge of the bandwidth of the transducer (4 MHz).

The release of fluorescein was thus confined to the focal region of the ultrasound where the acoustic pressure reaches substantial levels. The location of this focus could be changed by simply modifying the electronic delays applied on each element of the probe, an electronic process already exploited to produce the ultrasound images on conventional clinical scanners.

Figure 11 presents a 3 cm high representation of a landmark of Paris remotely printed in the culture plate by applying acoustic pulses point-by-point. The pattern was obtained through electronic delays in the vertical direction and, for practical reasons, using a motorized translating stage in the horizontal direction. Each line was created in 18 ms. This experiment demonstrated that the tattooed region where fluorescein is released could be easily seen by the naked eye. Figure 11 also indicated that the spatial resolution of our tattooing technique lies in the range 500–800 μm for typical ultrasonic frequencies used in clinical imaging.

III.C. *In vivo* proof-of-principle

In vivo tattooing was demonstrated in a chicken embryo. First, the complex droplets were injected in a vein of the CAM which is used as a model for the vascular system. The ultrasound array was focused on a specific spot on the vein far from the injection site during the first pass of the droplets. When 3.5 MPa pulses are directed toward the veins containing the composite droplets, a bright fluorescent spot appear within seconds (Fig. 12). This spot remained for at least 15 min until disposal of the egg and could be easily seen under blue illumination and orange photographic filters.

To demonstrate the circulation of the droplets and their remote spatially controlled release, 100 μl of the droplets

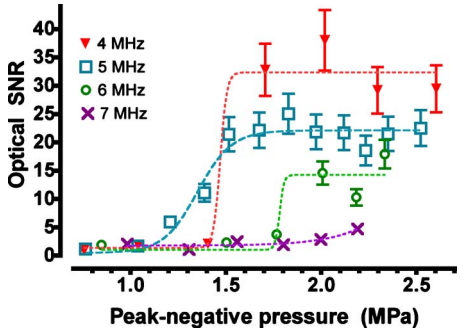

FIG. 10. Threshold values for the ultrasonic release at different frequencies using the same calibrated ultrasound multielement imaging probe. The fits are Boltzmann sigmoidal. The optic thresholds (P50) are 4 MHz, 1.47 MPa; 5 MHz, 1.35 MPa; 6 MHz, 1.78 MPa; and 7 MHz, 2.57 MPa.

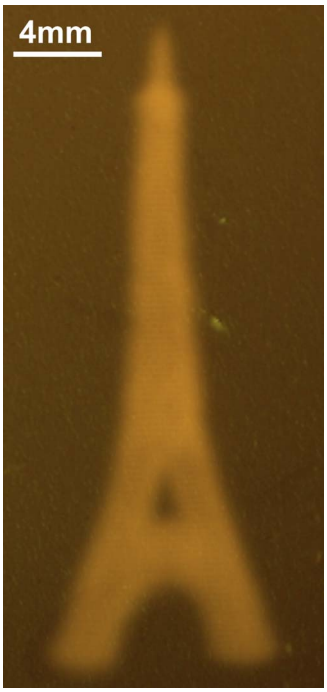

FIG. 11. Drawing made by moving the transducer within the Opticell plate. Photography made under blue illumination and with orange filters. The pattern is formed by the point-by-point release of fluorescein, as demonstrated by observations under fluorescent microscopy.

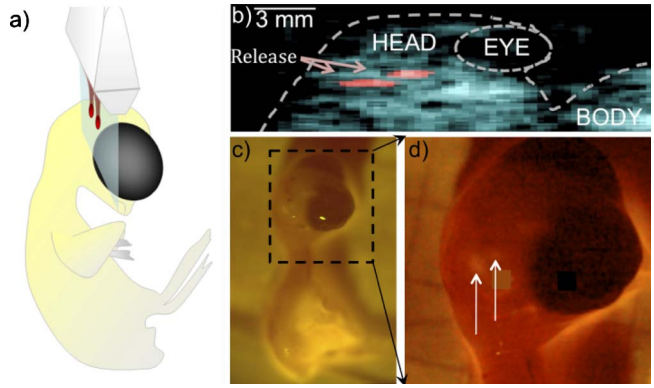

FIG. 13. Tattooing of two spots on the head of a chick embryo upon ultrasound release after intracardiac injection of the composite droplets. (a) Principle of the experiment. An ultrasound scan was obtained and two spots 2 mm apart were selected. [(c) and (d)] The photography showed the two spots on the embryo's head (white arrows). For visualization purposes, reflections on the head of the chick embryo were masked. (b) Acoustic signals due to the conversion of the droplets were shown as an overlay on the ultrasound scan itself. A 29 dB increase in echogenicity was observed at the site of release at the end of the 30 ms experiment.

suspension were injected inside the heart of 9 days chicken embryo. The droplets were left to circulate within the embryo before it was immersed under ultrasound coupling medium. The transducer array was aligned to obtain an axial image at the midline of the eye. Two spots 2 mm apart were selected for ultrasound-triggered release with acoustic pulses at 3.5 MPa peak-negative pressure [see sketch in Fig. 13(a)]. Concomitantly with the acoustic release, ultrafast ultrasound imaging was done to follow the effect of the droplets conversion. Within 300 μs, the two spots of controlled release were detectable on the ultrasound images representing fast changes in the acoustic echoes [overlay in Fig. 13(b)]. When the embryo was observed under blue light, the two spots were clearly detectable on the head of the embryo [see Figs. 13(c) and 13(d)].

Finally, to demonstrate ultrasound tattooing within tissue, part of the shell of a fertilized egg (9 days) was removed to create an acoustic and optical window. The composite droplets (100 μl) were injected within a vein of the chorioallantoique membrane. The droplets were left to circulate 5 min to the embryo itself. The egg was then immersed in water and ultrasound-induced release was performed at a focal spot near the eye of the embryo. Conversion was confirmed by ultrafast ultrasound imaging. Figure 14(a) shows the fluorescent spot on the embryo as observed through the chorioallantoique membrane and the allantoique cavity. The embryo was then removed from the shell, isolated on a culture plate, and observed under fluorescent light [Fig. 14(b)]. The spot was about 1 mm in diameter and lasted for the remainder of the experiment (30 min).

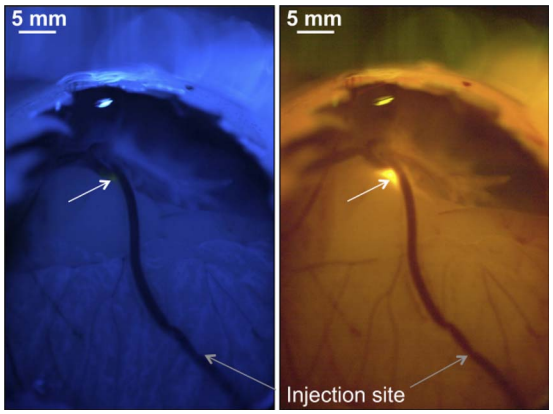

FIG. 12. Fluorescence imaging of the chorioallantoic membrane of an egg after release of fluorescence at the focus of the ultrasound beam (white arrows). Without (left) and with (right) the photographic filter

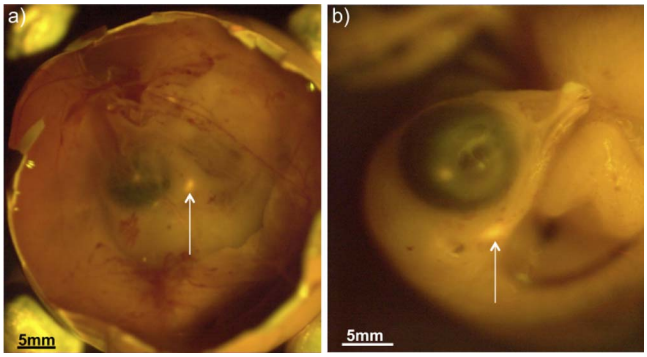

FIG. 14. Tattooing of one spot on the head of a chick embryo upon ultrasound release after injection of the composite droplets in a vein of the CAM. The photography showed the spot on the embryo's head (white arrows) (a) while the embryo is still in the egg and (b) once extracted from the shell and displayed in a Petri dish.

IV. DISCUSSION

The objective of this study was to design an ultrasound system as well as injectable agents such that a radiologist can tattoo a tissue that needs to be surgically resected. After the identification of diseased tissue during preoperative imaging, the agent would be injected intravenously and remotely deposited locally by an ultrasound system. The vector would release its staining content and make the region easily identifiable by the surgeon.

The large quantity of optical marker necessary for detection with the naked eye motivated the creation of a new kind of composite droplets for ultrasound delivery. These droplets contain a polydisperse nanoemulsion close to the maximum packing fraction. Thus, the internal aqueous phase forms more than two-thirds of the drops' volume, which can be saturated with markers currently used for angiography such as fluorescein or indocyanine green. In this study, the high concentrations of fluorescein induced an effect of quenching, a self-absorption of the fluorescent light. Consequently, the droplets do not induce a strong fluorescent signal until they are converted by ultrasound and thus ensure a strong spatial specificity of the tattooing approach. After this release, the fluorescence is very strong at the focus (Fig. 7). The proposed technology of ultrasound-activable composite droplets is characterized by key advantages.

First, the fluorinated intermediate liquid phase acts as a barrier, along with its more conventional[24] gas-precursor role. Indeed, except for oxygen,[25] most molecules have a very low solubility in perfluorocarbon and would not exchange between the external and internal phase. Since it was used for blood replacement and oxygen carrying, liquid perfluorocarbon's biocompatibility has been well characterized.[26] At optimum surfactant concentration, the content of the droplets is stabilized for several weeks. However, a water-in-perfluorocarbon-in-water drop is not naturally stable. Hence, specialized fluorinated surfactants are used to stabilize the nanoemulsion.

Second, the size of the droplets is easily controllable through the size of channels[20] in the microfluidic devices. The monodispersity of the droplets has two advantages. First, it prevents embolization caused by larger droplets that are necessarily present in agents with a broad size distribution. Also, microagents react to ultrasound based on their size and the acoustic frequency. Monodispersity guarantees that all agents convert at the same pressure, which was confirmed by the step threshold observed in Fig. 9. Such a threshold phenomenon allows a precise control over the region where the droplets are converted.

Third, the technology for local delivery already exists on most clinical ultrasound scanner. With appropriate control over the electronic, an ultrasound probe can be made to focus a precise amount of ultrasound dose at a location defined by the user. The spatial resolution is defined by the acoustic frequency and is below 300 μm for 5 MHz probe typically used for abdominal imaging. As in the case of the Eiffel Tower in Fig. 11, the delivery zone can be created point-by-point by moving the focal zone. Conversion of the drops is determined by the peak-negative pressure attained in the focal region of the transducer. The ultrasound pulse induces the vaporization or cavitation of the perfluorocarbon content and its separation from its aqueous inclusions (Fig. 7). The hydrophilic content is thus freed from the droplets by phenomena that could possibly combine cavitation, vaporization, and mechanical effects within the droplets. However, the exact process will have to be further studied. Interestingly, for our droplets, these events took place at acoustic pressures well within clinical limits for imaging and for single-cycle pulses (0.2 μs in length). The effect of single-cycle pulses demonstrate that the conversion of the droplets is not due to thermal effect, but rather to the pressure change induced by ultrasound. A clinical ultrasound scanner could thus perform the preoperative imaging and deliver the optical markers. The fact that such tattooing is activated during ultrasonic imaging by the same conventional probe that performs the patient exam is also a key advantage of our approach. Indeed, such point ensures the perfect colocalization between the ultrasonic radiological image and the spatial delivery of optical markers *in situ*. Finally, the use of ultrafast ultrasonic imaging sequences could also enable the direct visualization of the droplets release on the ultrasonic image.

The concept of internal tattooing also requires the optical markers to penetrate in the extravascular medium, so that they are not simply eliminated by blood flow. This process can be induced by the formation of pores on cells by the interaction of the agents with ultrasound.[9] Although the fluorescent spots in Figs. 13 and 14 remained until disposal of the chicken embryo, such sonoporation as yet to be studied. More work also has to be done on the biocompatibility of the droplets and their survival to the immune system of an adult animal.

The technology of ultrasound-inducible droplets presents key differentiators such as a large carrier payload, a stable formulation, a low diffusion in the external medium, and a monodisperse size distribution resulting in a sharp activation threshold. Most importantly, the large payload and the confinement of the content of the ultrasound-inducible droplets can contribute to medicine in a much broader sense than just internal tattooing. Their flexible design would allow the straightforward addition of other types of markers such as gadolinium, iron oxide, and iodine to the hydrophilic phase. Moreover, high concentrations of chemotherapeutic agents could be delivered through these composite particles under ultrasound guidance. More interestingly, some ultrasound-activable drugs could be designed, reducing significantly the dose to healthy tissue outside of the focal zone. Finally, transporting and transfecting DNA or RNA to a specific site, while being protected from enzymes in the blood, could be highly beneficial to genetic therapies.[27]

ACKNOWLEDGMENTS

The authors thank Laurent Boitard and Fabien Bertholle for their help with the fluorinated surfactant.

[a]Author to whom correspondence should be addressed. Electronic addresses: olivier.couture@espci.fr and olicou@gmail.com; Telephone: (33) 06 50 87 08 96.

[1]S. Benoist, A. Brouquet, A. Penna, C. Julie, M. El Hajjam, S. Chagnon, E. Mitry, P. Rougier, and B. Nordlinger, "Complete response of colorectal liver metastases after chemotherapy: Does it mean cure?," J. Clin. Oncol. **24**, 3939–3945 (2006).

[2]E. Kouskos, G. P. Gui, D. Mantas, K. Revenas, N. Rallis, Z. Antonopoulos, E. Lampadariou, H. Gogas, and C. Markopoulos, "Wire localisation biopsy of non-palpable breast lesions: Reasons for unsuccessful excision," Eur. J. Gynaecol. Oncol. **27**, 262–266 (2006).

[3]S. Van Esser, M. Hobbelink, I. M. Van der Ploeg, W. P. Mali, P. J. Van Diest, I. H. Borel Rinkes, and R. Van Hillegersberg, "Radio guided occult lesion localization (ROLL) for non-palpable invasive breast cancer," J. Surg. Oncol. **98**, 526–529 (2008).

[4]Y. Z. Wang, J. P. Boudreaux, A. Dowling, and E. A. Woltering, "Percutaneous localisation of pulmonary nodules prior to video-assisted thoracoscopic surgery using methylene blue and TC-99," Eur. J. Cardiothorac Surg. **37**, 237–238 (2010).

[5]T. P. Rauth, P. Q. Bao, R. L. Galloway, J. Bieszczad, E. M. Friets, D. A. Knaus, D. B. Kynor, and A. J. Herline, "Laparoscopic surface scanning and subsurface targeting: Implications for image-guided laparoscopic liver surgery," Surgery (St. Louis) **142**, 207–214 (2007).

[6]K. J. Oldhafer, G. A. Stavrou, G. Prause, H.-O. Peitgen, C. T. Lueth, and S. Weber, "How to operate a liver tumor you cannot see," Langenbecks Arch. Surg. **394**, 489–494 (2009).

[7]A. Nakayama, F. del Monte, R. J. Hajjar, and J. V. Frangioni, "Functional near-infared fluorescence imaging for cardiac surgery and targeted gene therapy," Mol. Imaging **1**, 365–377 (2002).

[8]S. L. Troyan, V. Kianzad, S. L. Gibbs-Strauss, S. Gioux, A. Matsui, R. Oketokoun, L. Ngo, A. Khamene, F. Azar, and J. V. Frangioni, "The FLARE intraoperative near-infared fluorescence imaging system: A first-in-human clinician trial in breast cancer sentinel lymph node mapping," Ann. Surg. Oncol. **16**, 2943–2952 (2009).

[9]R. Karshafian, P. D. Bevan, R. Williams, S. Samac, and P. N. Burns, "Sonoporation by ultrasound-activated microbubble contrast agents," Ultrasound Med. Biol. **35**, 847–860 (2009).

[10]M. Postema and O. H. Gilja, "Ultrasound-directed drug delivery," Curr. Pharm. Biotechnol. **8**, 355–361 (2007).

[11]O. Couture, N. Pannacci, A. Babataheri, P. Tabeling, M. Fink, V. Servois, and M. Tanter, "Ultrasound-inducible fluorescent particles for internal tattooing," in Proceedings of the IEEE Ultrasonics Symposium, Rome, Italy, 2009 (unpublished).

[12]K. Kawabata, N. Sugita, H. Yoshikawa, T. Azuma, and S. Umemura, "Nanoparticles with multiple perfluorocarbons for controllable ultrasonically induced phase shifting," Jpn. J. Appl. Phys., Part 1 **44**, 4548–4552 (2005).

[13]N. Rapoport, D. A. Christensen, A. M. Kennedy, and K. H. Nam, "Cavitation properties of block copolymer stabilized phase-shift nanoemulsions used as drug carriers," Ultrasound Med. Biol. **36**, 419–429 (2010).

[14]K. C. Schad and K. Hynynen, "In vitro characterization of perfluorocarbon droplets for focused ultrasound therapy," Phys. Med. Biol. **55**, 4933–4947 (2010).

[15]T. Giesecke and K. Hynynen, "Ultrasound-mediated thresholds of liquid perfluorocarbon droplets in vitro," Ultrasound Med. Biol. **29**, 1359–1365 (2003).

[16]M. Seo, I. Gorelikov, R. Williams, and N. Matsuura, "Microfluidic assembly of monodisperse, nanoparticle-incorporated perfluorocarbon microbubbles for medical imaging and therapy," Langmuir **26**, 13855–13860 (2010).

[17]O. D. Kripfgans, J. B. Fowlkes, D. L. Miller, O. P. Eldevik, and P. L. Carson, "Acoustic droplet vaporization for therapeutic and diagnostic applications," Ultrasound Med. Biol. **26**, 1177–1189 (2000).

[18]M. L. Fabiilli, K. J. Haworth, N. H. Fakhri, O. D. Kripfgans, P. L. Carson, and J. B. Fowlkes, "The role of inertial cavitation in acoustic droplet vaporization," IEEE Trans. Ultrason. Ferroelectr. Freq. Control **56**, 1006–1017 (2009).

[19]C. Holtze, A. Rowat, J. Agresti, J. Hutchison, F. Angilé, C. Schmitz, S. Koster, H. Duan, K. Humphry, and R. Scanga, "Biocompatible surfactants in water-in-fluorocarbons emulsions," Lab Chip **8**, 1632–1639 (2008).

[20]F. Malloggi, N. Pannacci, R. Attia, F. Monti, P. Mary, H. Willaime, and P. Tabeling, "Monodisperse colloids synthesized with nanofluidic technology," Langmuir **26**, 2369–2373 (2010).

[21]G. Montaldo, M. Tanter, J. Bercoff, N. Benech, and M. Fink, "Coherent plane-wave compounding for very high frame rate ultrasonography and transient elastography," IEEE Trans. Ultrason. Ferroelectr. Freq. Control **56**, 489–506 (2009).

[22]R. S. Knox, "Theory of polarization quenching by excitation transfer," Physica (Amsterdam) **39**, 361–386 (1968).

[23]O. Couture, S. Bannouf, F. Montaldo, J. F. Aubry, M. Fink, and M. Tanter, "Ultrafast imaging of ultrasound contrast agents," Ultrasound Med. Biol. **35**, 1908–1916 (2009).

[24]E. C. Unger, T. Porter, W. Culp, R. Labell, T. Matsunaga, and R. Zutschi, "Therapeutic applications of lipid-coated microbubbles," Adv. Drug Delivery Rev. **56**, 1291–1314 (2004).

[25]J. G. Riess and M. P. Krafft, "Advanced fluorocarbon-based systems for oxygen and drug delivery and diagnosis," Artif. Cells Blood Substit Immobil Biotechnol. **25**, 43–52 (1997).

[26]J. G. Riess, "Fluorine in our arteries," New J. Chem. **19**, 891–909 (1995).

[27]R. Suzuki, T. Takizawa, Y. Negishi, N. Utoguchi, and K. Maruyama, "Effective gene delivery with novel liposomal bubbles and ultrasonic destruction technology," Int. J. Pharm. **354**, 49–55 (2008).